Supporting Information

Tailoring the Mechanical Properties of Benzothiadiazole-Based Semiconducting Polymers through Chalcogen Atom Substitution

Piumi Kulatunga,[1] Marc Comí,[2] Tiago Carneiro Gomes,[1] Moutasem Seifi,[1] Robabeh Majidzadeh,[1] Mohammed Al-Hashimi,[2] and Simon Rondeau-Gagné *[1]*

[1] Department of Chemistry and Biochemistry, Advanced Materials Centre of Research, University of Windsor, Windsor, ON, Canada N9B 3P4.

[2] Department of Chemistry, Texas A&M University at Qatar, Education City, Doha, P.O. Box 23874, Qatar.

Correspondence should be addressed to:

* Prof. Simon Rondeau-Gagné (srondeau@uwindsor.ca)

* Mohammed Al-Hashimi, email: mohammed.al-hashimi@tamu.edu

Contents

Materials and Methods

All commercially available solvents, reagents, and chemicals were used as received without further purification unless otherwise stated. Anhydrous solvent tetrahydrofuran was distilled from sodium under argon. 4,7-Dibromo-5,6-difluorobenzo[*c*][1,2,5]thiadiazole, 2-octan-1-ol, sodium *tert*-butoxide, *N*-bromosuccinimide were purchased from Sigma Aldrich. Unless otherwise stated all operations and reactions were carried out under argon using standard Schlenk line techniques. ^{1}H spectrum was recorded on a Bruker AV-400 (400 MHz), using the residual solvent resonance of $CDCl_3$ or TMS as an internal reference and are given in ppm. Number-average molecular weight (M_n) and weight average molecular weight (M_w) were determined by Agilent Technologies 1200 series GPC running in chlorobenzene at 85 °C, using two PL mixed B columns in series, and calibrated against narrow polydispersity polystyrene standards. UV-visible spectroscopy was performed on a Varian UV/Visible Cary 50 spectrophotometer. Flash chromatography (FC) was performed on silica gel (Merck Kieselgel 60 F254 230-400 mesh) unless otherwise indicated. Thin Layer Chromatography (TLC) was performed on Merck aluminum-backed plates pre-coated with silica (0.2 mm, 60 F254). Microwave experiments were performed in a Biotage initiator V 2.3. The surface structure of polymer film was obtained using a Multimode atomic force microscope (AFM, Digital Instruments) operated in the tapping mode at room temperature. Images were collected using Nanoscope 6 software and processed using Gwyddion software. All the measurements of the transistors were conducted using a Keithley 4200 semiconductor parameter analyzer (Keithley Instruments Inc.) under dry N_2 (glovebox) and at room temperature.

Transfer-Printed Organic Field-Effect Transistor Fabrication

To measure the charge mobilities upon stretching, a lamination procedure adapted from previous literature was used to laminate the semiconducting polymer films onto PDMS. The resulting thin films supported on PDMS were stretched to 0%, 10%, 20%, and 30% strain, and laminated back to Si wafers. Source and drain top electrodes were deposited parallel and perpendicular to the stretching direction by evaporating gold (≈ 50 nm) through a shadow mask with a channel length (L) and width (W) defined as 100 and 1000 μm, respectively. All measurements were conducted using a Keithley 4200-SCS semiconductor parameter analyzer (Keithley Instruments Inc., Cleveland, OH, USA) in an N_2 filled glove box at room temperature. Polymers were dissolved in 10mg/mL Chlorobenzene.

Experimental Procedure

In a microwave vial equimolar amounts of monomer **(**0.20 mmol) and bis(trimethylstannyl) [thiophene (**P1**) or selenophene (**P2**) or bithiophene (**P3**) or biselenophene (**P4**) were dissolved in anhydrous chlorobenzene (0.5 mL) followed by addition of tetrakis(triphenylphosphine)palladium (2 mol%, 5.02 mg), the resultant mixture was degassed for 30 min with argon and securely sealed. The glass vial was placed into a microwave reactor and heated at 140 °C for 2 min, 160 °C for 2 min, and followed by 180 °C for 30 min. After being cooled to room temperature, the reaction mixture was precipitated into a mixture of methanol (200 mL) and concentrated HCl (2 mL) and stirred for 1 h at RT. The precipitate was filtered and extracted (Soxhlet) with methanol, acetone, n-hexane, chloroform. The remaining polymer was dissolved in chlorobenzene and precipitated into methanol, filtered and dried under vacuum to achieve the desired polymers as a dark purple solid. The ^{1}H NMR spectrum for all polymers exhibited considerable broadening of the aromatic

and methylene peaks and only alkyl sidechain protons were observable. The full characterization for polymers **P1** to **P3** can be found in previous reports.[1] The list of NMR peaks for all polymers have been included below.

P1: Yield 95 mg, ^{1}H NMR (400 MHz, $CDCl_3$) δ 8.48 (2H), 7.71 (1H), 7.53 (1H), 4.21 (4H), 2.92 (4H), 2.02 (4H), 1.82 (4H), 1.20-1.60 (40H), 0.89 (12H); GPC: M_n = 42,400 g/mol, $Đ$ =2.1; UV-vis: λ_{max} = 565 nm (dilute chlorobenzene solution).

P2: Dark Purple, Yield 95 mg, ^{1}H NMR (400 MHz, $CDCl_3$) δ 8.47 (2H), 7.72 (1H), 7.53 (1H), 4.21 (4H), 2.95 (4H), 2.02 (4H), 1.81 (4H), 1.20-1.60 (40H), 0.89 (12H); GPC: M_n = 46,200 g/mol, $Đ$ =2.0; UV-vis: λ_{max} = 551 nm (dilute chlorobenzene solution).

P3: Dark Purple, Yield 95 mg, ^{1}H NMR (400 MHz, $CDCl_3$) δ 8.47 (2H), 7.72 (1H), 7.51 (1H), 7.42 (2H), 4.22 (4H), 2.92 (4H), 2.02 (4H), 1.82 (4H), 1.20-1.60 (40H), 0.89 (12H); GPC: M_n = 39,600g/mol, $Đ$ =1.9 UV-vis: λ_{max} = 551 nm (dilute chlorobenzene solution).

P4: Dark Purple, Yield 95 mg, ^{1}H NMR (400 MHz, $CDCl_3$) δ 8.47 (2H), 7.73 (1H), 7.52 (1H), 4.20(4H), 2.95 (4H), 2.02 (4H), 1.81 (4H), 1.20-1.60 (40H), 0.89 (12H); GPC: M_n = 41,200 g/mol, $Đ$ =2.0; UV-vis: λ_{max} = 551 nm (dilute chlorobenzene solution).

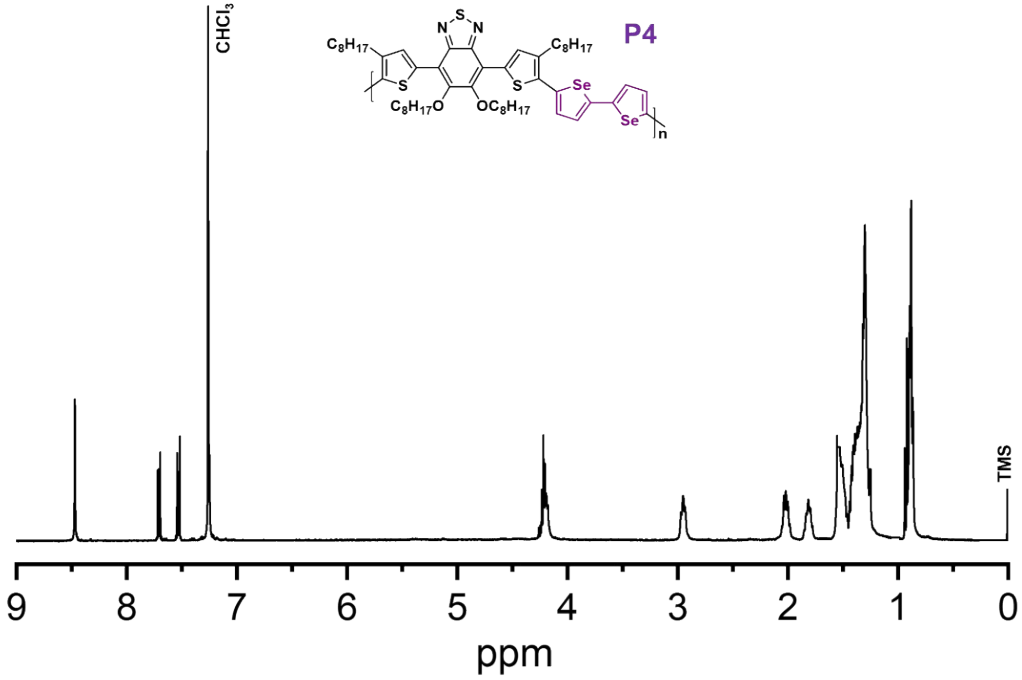

Figure S1. ^{1}H NMR spectrum of **P4** in $CDCl_3$

Materials Characterization

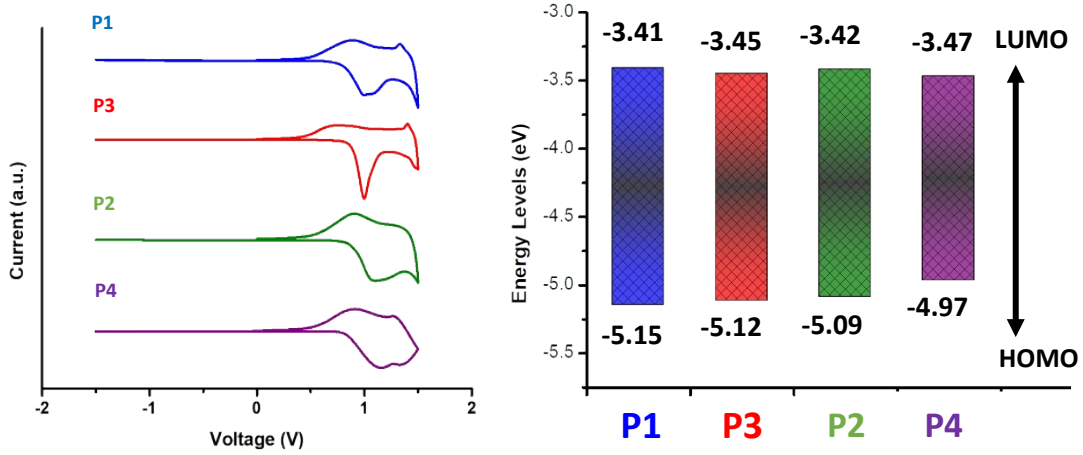

Figure S2: (a) Cyclic voltammograms of **P1–P4** as thin film (scan rate 50 mV s-1, (b) HOMO and LUMO energy levels of the copolymers **P1–P4**.

Optical and structure properties

Table S1: Summary of molecular weights, optical, and electrochemical, copolymers **P1–P4**

Sample	M_n (kDa)	Đ	HOMO (eV)	LUMO (eV)	E_g^{el} (eV)
P1	42	2.1	-5.15	-3.41	1.74
P2	40	2.0	-5.09	-3.42	1.67
P3	46	1.9	-5.12	-3.45	1.67
P4	41	2.1	-4.97	-3.47	1.50

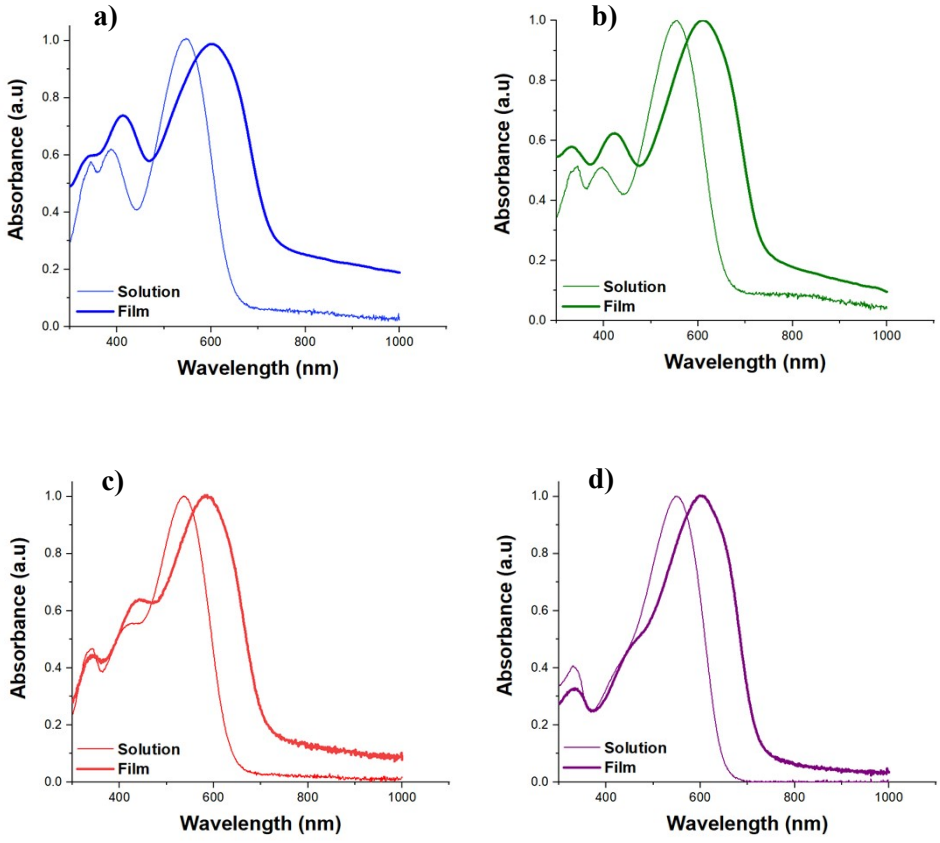

Figure S3. UV-vis absorption spectra in solution (chlorobenzene) and thin films spin-coated on SiO_2 for a) **P1**, b) **P2**, c) **P3**, and (d) **P4**.

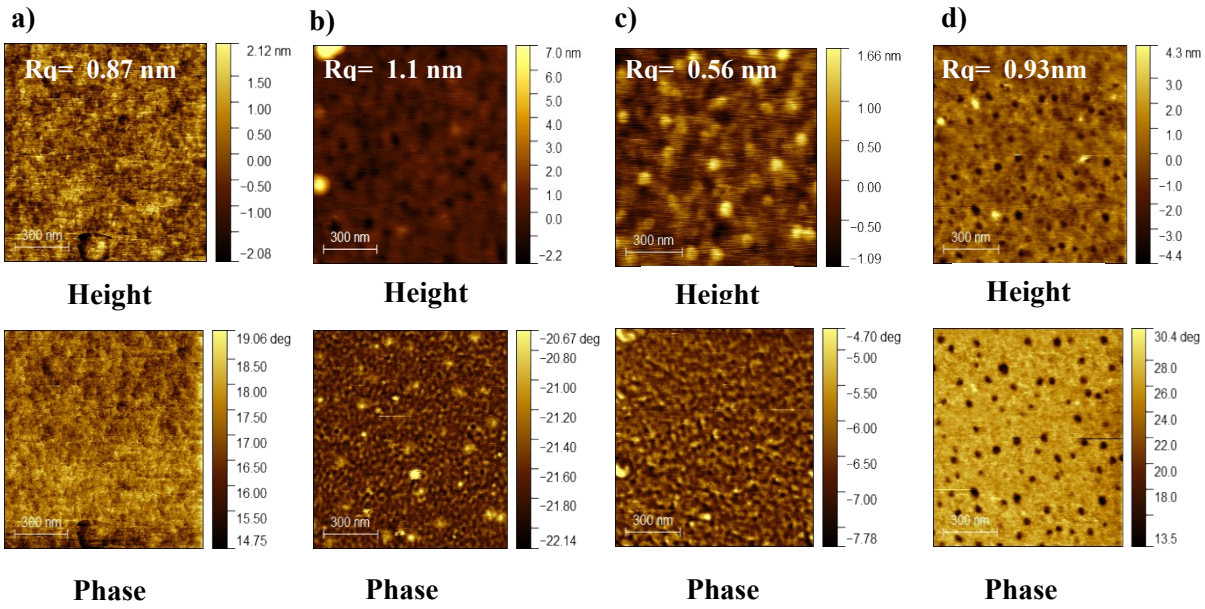

Figure S4. Atomic-force microscopy (tapping mode) height and phase images of a) **P1**, b) **P2**, c) **P3** and d) **P4**. Scale bar is 300 nm.

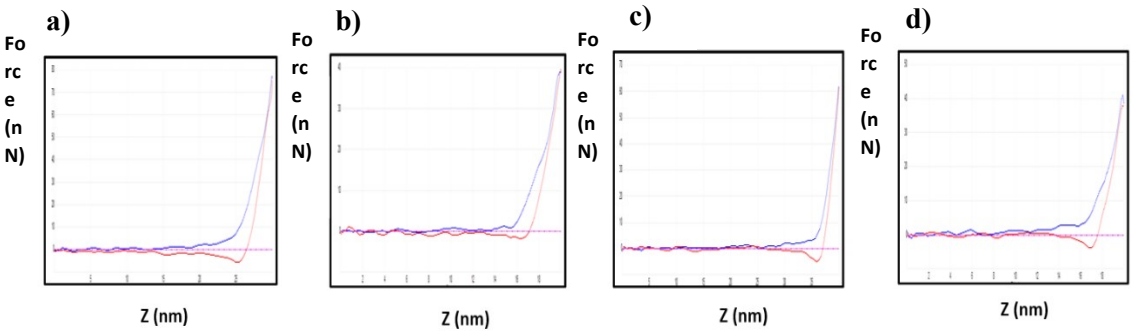

Figure S5. DMT modulus Force curves for a) **P1**, b) **P2**, c) **P3**, and d) **P4**.

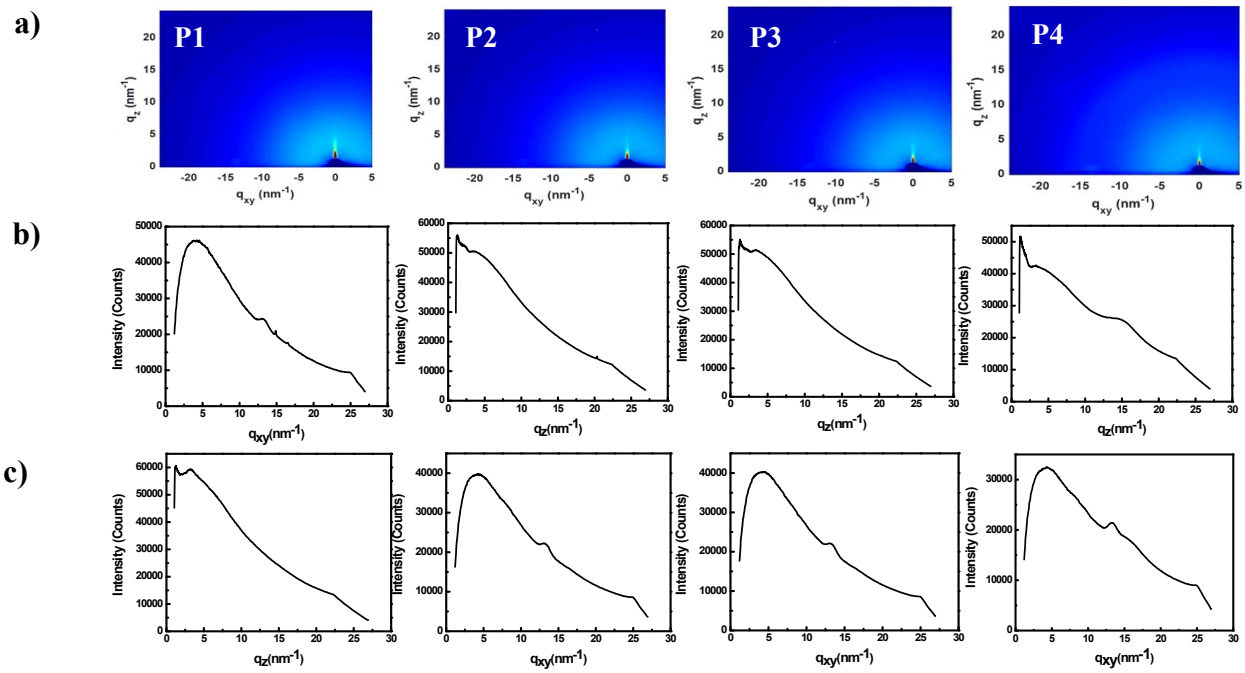

Figure S6. GIWAXS 2D patterns of (a) **P1-P4**, ID scattering profiles (b) out of plane and (c) in plane profiles, obtained from 2D GIWAXS data.

Charge transport properties in OFETs upon strain

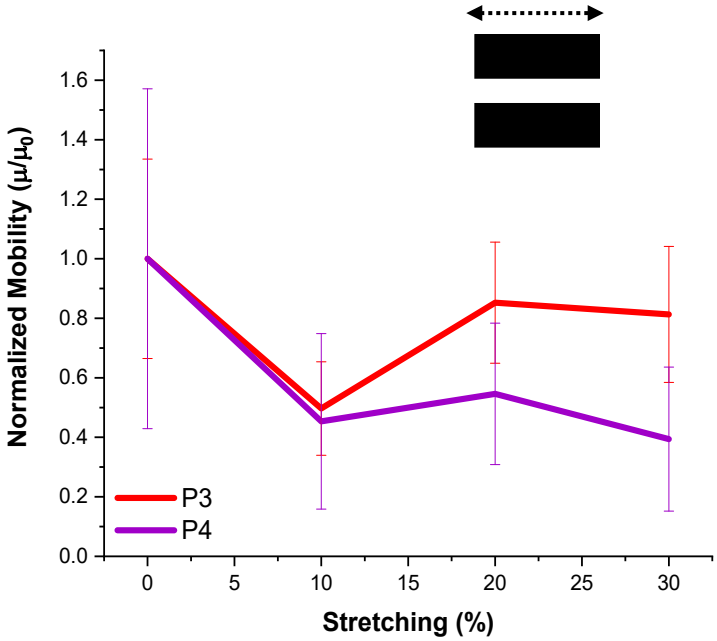

Figure S7: Mobility values of stretched films for **P3** and **P4** normalized by initial values at 0% strain for charge transport oriented perpendicular to strain direction.

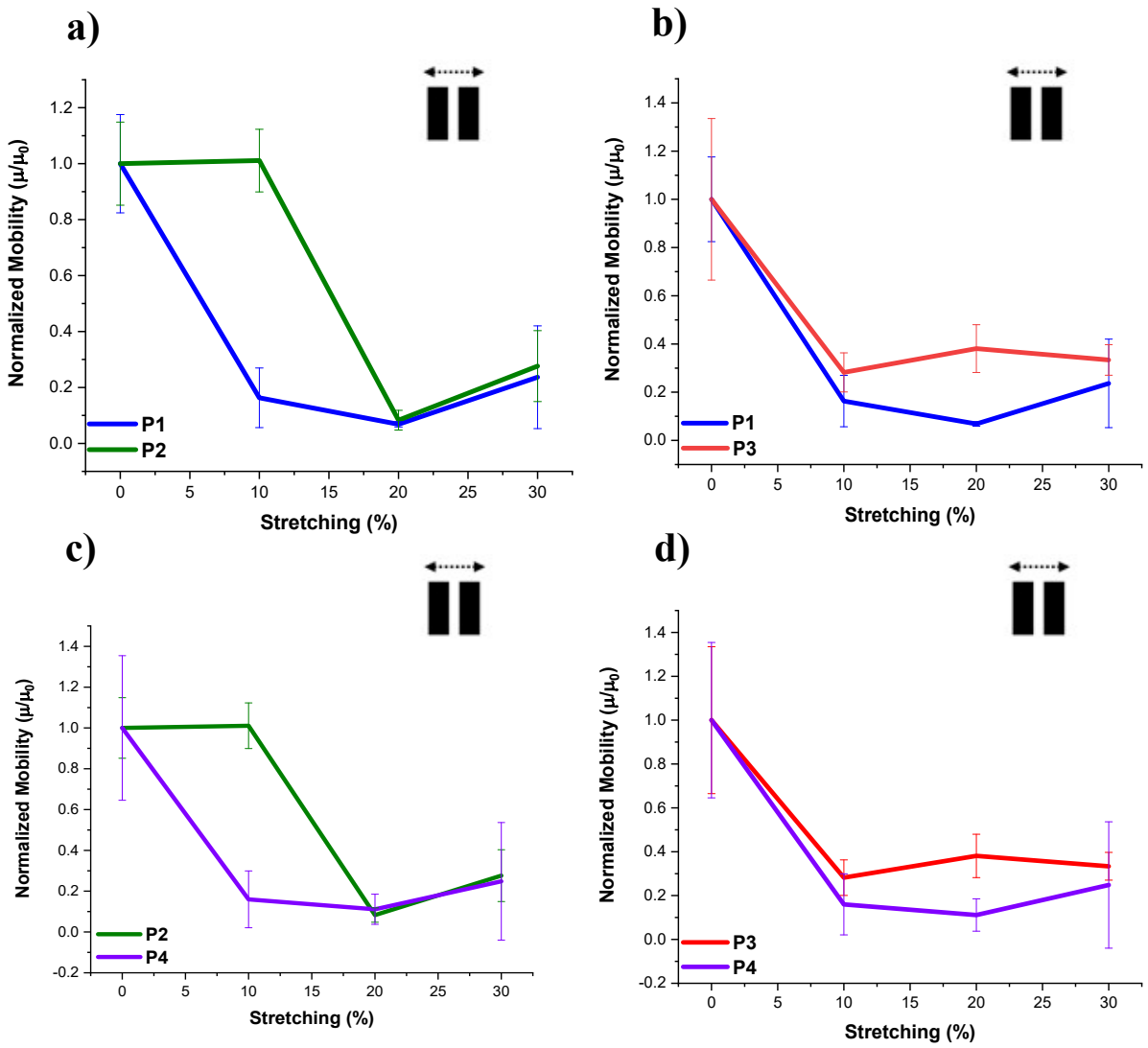

Figure S8: Mobility values of stretched films for **P1** to **P4** normalized by initial values at 0% strain for charge transport oriented parallel to strain direction. (a) **P1** and **P2** (b) **P1** and **P3** (c) **P2** and **P4**, (d) **P3** and **P4**.

Table S3. Average (μ_h^{avg}) and maximum hole mobilities (μ_h^{max}), threshold voltages (V_{th}), I_{ON}/I_{OFF} ratios for OFETs fabricated using pre-stretched (0 and 25% strain) polymer blend films (0 to 50 wt.% LPE). The device performances were averaged from 5 devices and W/L represents channel width/length.

Sample	Direction	Strain %	W/L	μ_h^{avg}/μ_h^{max} ($cm^2 V^{-1} s^{-1}$)	I_{ON}/I_{OFF}^{avg}	V_{th}^{avg} (V)
P1	Perpendicular	0	10	$6.7x10^{-5} \pm 5.8x10^{-5}/ 7.3x10^{-5}$	10^1	-11.2 ±0.8
		10		$1.7x10^{-5} \pm 4.3x10^{-5}/ 2.2x10^{-5}$	10^1	-12.9 ±1.9
		20		$8.6x10^{-6} \pm 7.9x10^{-5}/ 2.1x10^{-5}$	10^2	-17.4 ±7.2
		30		$1.1x10^{-5} \pm 5.4x10^{-5}/ 1.6x10^{-5}$	10^2	-15.7 ±1.5
	Parallel	0	10	$6.7x10^{-5} \pm 5.8x10^{-6}/ 7.3x10^{-5}$	10^1	-11.2 ±0.8
		10		$1.1x10^{-5} \pm 6.1x10^{-6}/ 1.8x10^{-5}$	10^1	-15.2 ±1.3
		20		$4.6x10^{-6} \pm 2.1x10^{-7}/ 4.8x10^{-6}$	10^1	-17.4 ±4.4
		30		$1.6x10^{-5} \pm 1.1x10^{-5}/ 3.5x10^{-5}$	10^1	-15.8 ±2.1
P2	Perpendicular	0	10	$5.1x10^{-5} \pm 9.1x10^{-6}/ 5.9x10^{-5}$	10^1	-11.2 ±1.3
		10		$1.9x10^{-5} \pm 3.3x10^{-6}/ 2.4x10^{-5}$	10^1	-11.6 ±2.2
		20		$1.6x10^{-5} \pm 9.1x10^{-6}/ 2.8x10^{-5}$	10^1	-7.1 ±0.6
		30		$1.6x10^{-5} \pm 2.4x10^{-6}/ 1.8x10^{-5}$	10^1	-11.8 ±0.9
	Parallel	0	10	$5.1x10^{-5} \pm 3.1x10^{-6}/ 5.9x10^{-5}$	10^1	-11.2 ±1.3
		10		$9.1x10^{-6} \pm 1.8x10^{-6}/ 1.1x10^{-5}$	10^1	-9.8 ±1.4
		20		$4.7x10^{-6} \pm 8.3x10^{-6}/ 6.2x10^{-6}$	10^1	-7.8 ±2.8
		30		$1.3x10^{-5} \pm 3.8x10^{-6}/ 2.3x10^{-5}$	10^1	-15.2 ±0.7
P3	Perpendicular	0	10	$7.7x10^{-5} \pm 1.2x10^{-6}/ 9.2x10^{-5}$	10^1	-25.3 ±0.5
		10		$3.8x10^{-5} \pm 5.5x10^{-6}/ 4.6x10^{-5}$	10^1	-18.3 ±0.8
		20		$6.5x10^{-5} \pm 4.5x10^{-6}/ 7.1x10^{-5}$	10^1	-28.6 ±0.9
		30		$6.2x10^{-5} \pm 6.9x10^{-6}/ 6.8x10^{-5}$	10^2	-27.1 ±1.2
	Parallel	0	10	$7.7x10^{-5} \pm 1.2x10^{-5}/ 9.2x10^{-5}$	10^1	-25.3 ±0.5
		10		$2.2x10^{-5} \pm 2.5x10^{-6}/ 2.3x10^{-5}$	10^1	-24.2 ±1.4
		20		$2.9x10^{-5} \pm 2.6x10^{-6}/ 3.2x10^{-5}$	10^1	-27.2 ±4.1
		30		$2.6x10^{-5} \pm 5.6x10^{-7}/ 2.6x10^{-5}$	10^1	-25.2 ±0.8
P4	Perpendicular	0	10	$1.7x10^{-4} \pm 2.8x10^{-5}/ 1.9x10^{-4}$	10^2	-11.2 ±1.6
		10		$6.8x10^{-5} \pm 2.3x10^{-6}/ 9.4x10^{-5}$	10^2	-7.9 ±1.9
		20		$8.3x10^{-5} \pm 1.1x10^{-6}/ 9.5x10^{-5}$	10^2	-5.6 ±2.9
		30		$6.2x10^{-5} \pm 1.3x10^{-6}/ 8.1x10^{-5}$	10^2	-5.1 ±3.2
	Parallel	0	10	$1.7x10^{-4} \pm 9.8x10^{-6}/ 1.2x10^{-5}$	10^2	-11.2 ±1.6
		10		$1.8x10^{-4} \pm 1.8x10^{-6}/ 6.8x10^{-6}$	10^2	-10.2 ±3.4
		20		$3.3x10^{-5} \pm 1.6x10^{-6}/ 9.6x10^{-6}$	10^2	-8.6 ±4.1
		30		$4.6x10^{-5} \pm 6.9x10^{-6}/ 2.1x10^{-5}$	10^2	-7.2 ±3.1

Output and transfer curves of OFETs upon strain

Strain for charge transport oriented perpendicular to strain direction - **P1**

a)

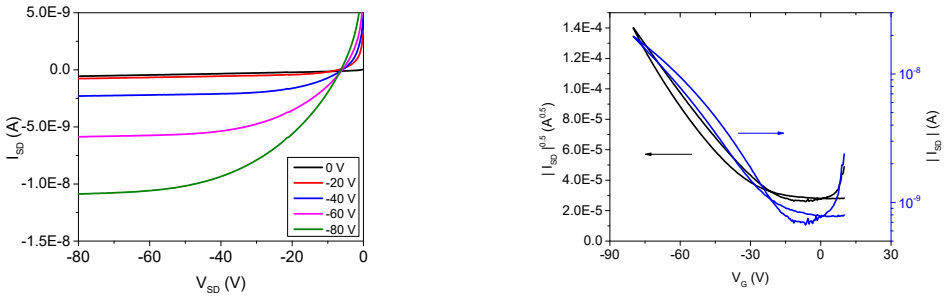

b)

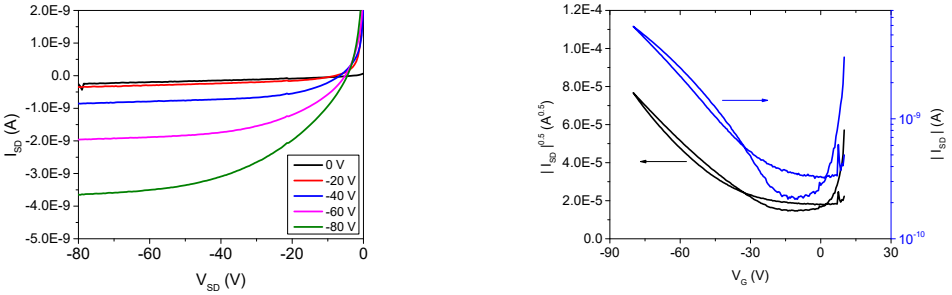

c)

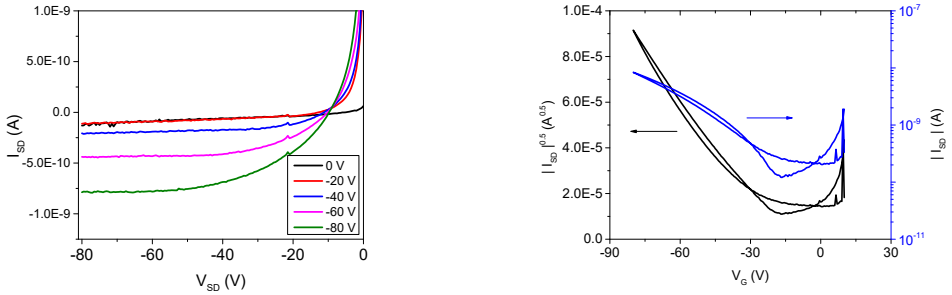

d)

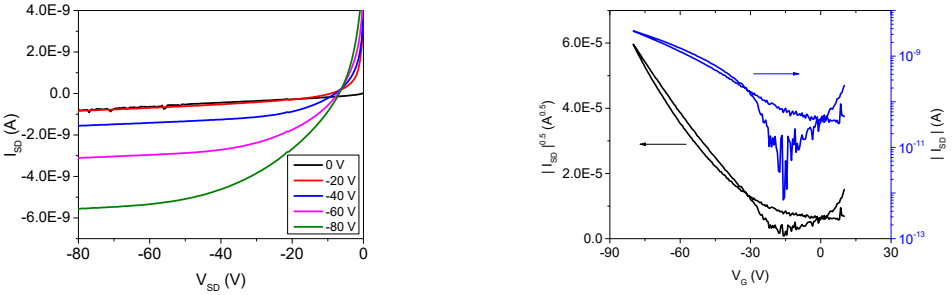

Figure S9: Representative OFET characteristics devices prepared from **P1** on SiO_2. a) output (left) and transfer (right) curves for devices at a) 0%, b) 10%, c) 20% and d) 30% strain for charge transport oriented perpendicular to strain direction.

<u>Strain for charge transport oriented parallel to strain direction - **P1**</u>

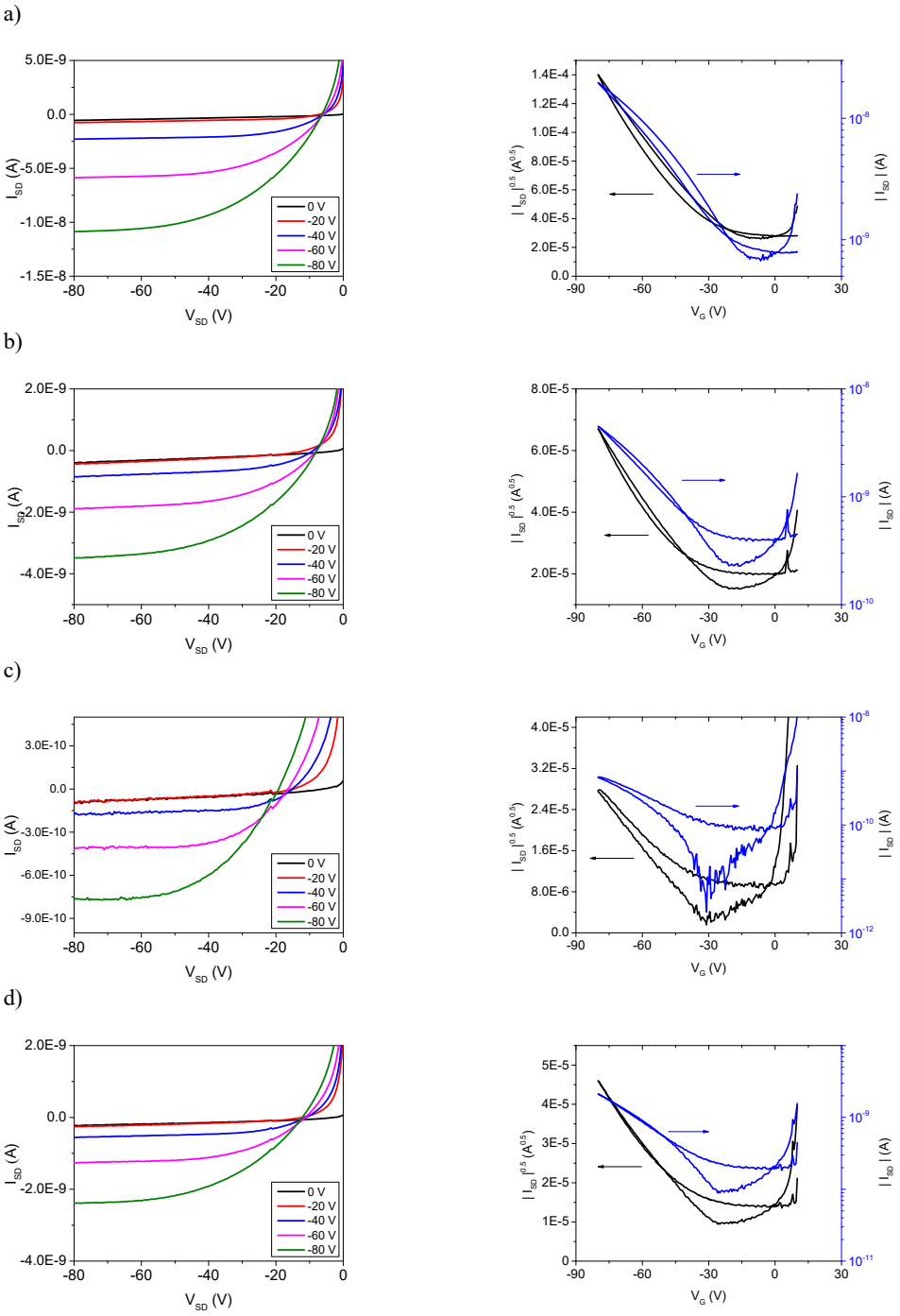

Figure S10: Representative OFET characteristics devices prepared from P1 on SiO_2. a) output (left) and transfer (right) curves for devices at a) 0%, b) 10%, c) 20% and d) 30% strain for charge transport oriented parallel to strain direction.

<u>Strain for charge transport oriented perpendicular to strain direction - **P2**</u>

a)

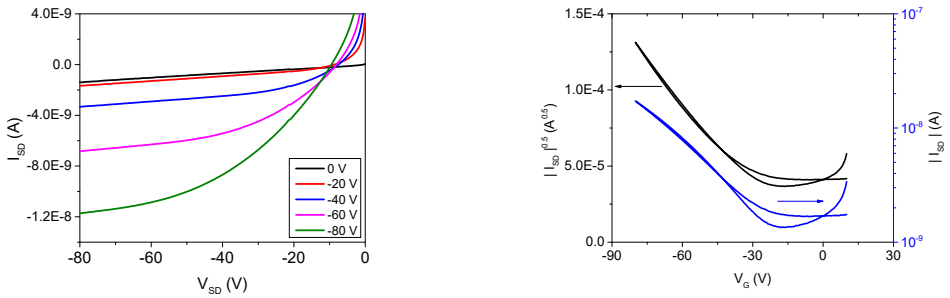

b)

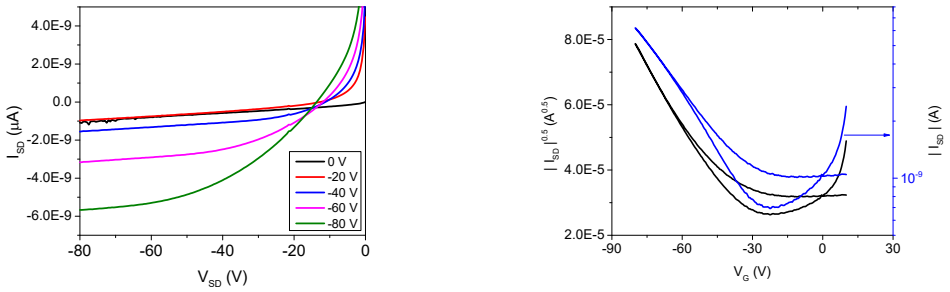

c)

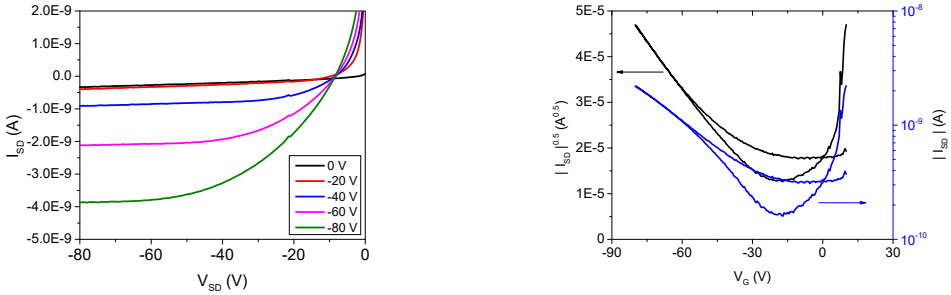

d)

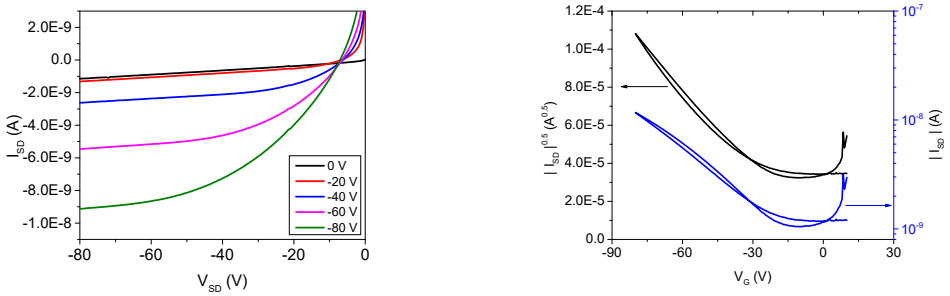

Figure S11: Representative OFET characteristics devices prepared from P2 on SiO_2. a) output (left) and transfer (right) curves for devices at a) 0%, b) 10%, c) 20% and d) 30% strain for charge transport oriented perpendicular to strain direction.

Strain for charge transport oriented parallel to strain direction - **P2**

a)

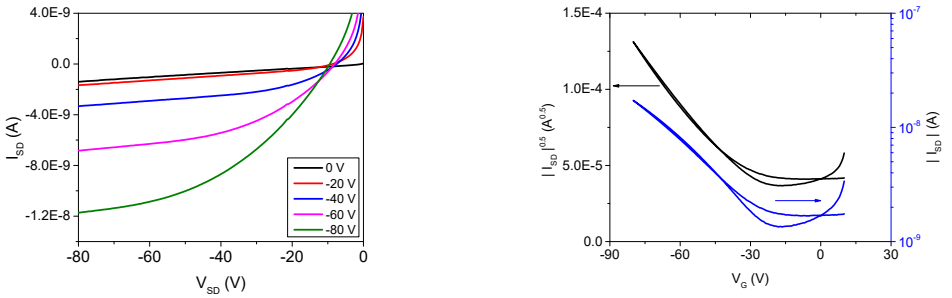

b)

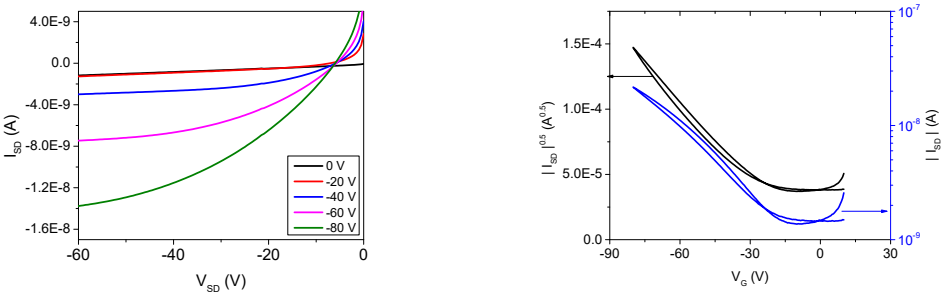

c)

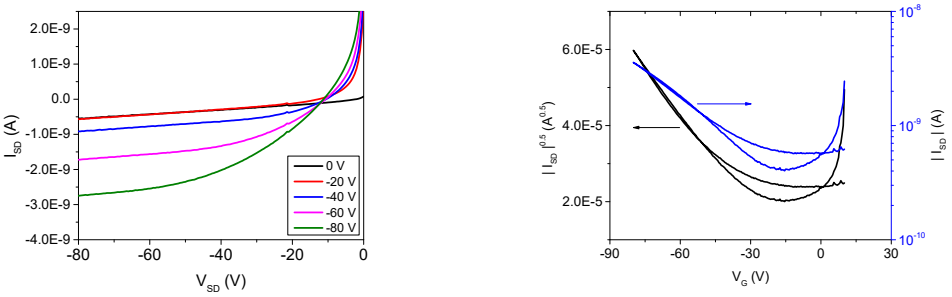

d)

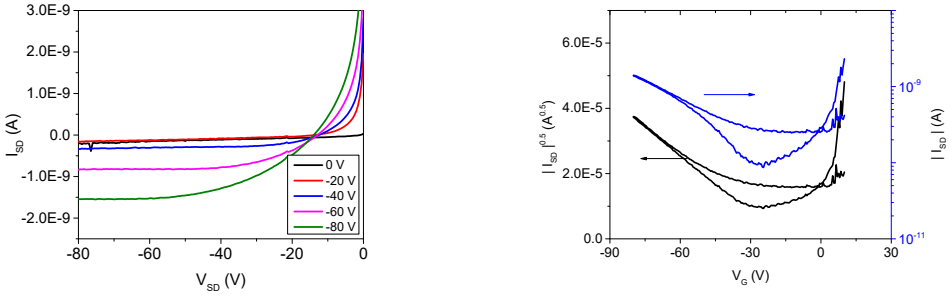

Figure S12: Representative OFET characteristics devices prepared from P2 on SiO_2. a) output (left) and transfer (right) curves for devices at a) 0%, b) 10%, c) 20% and d) 30% strain for charge transport oriented parallel to strain direction.

Strain for charge transport oriented perpendicular to strain direction - **P3**

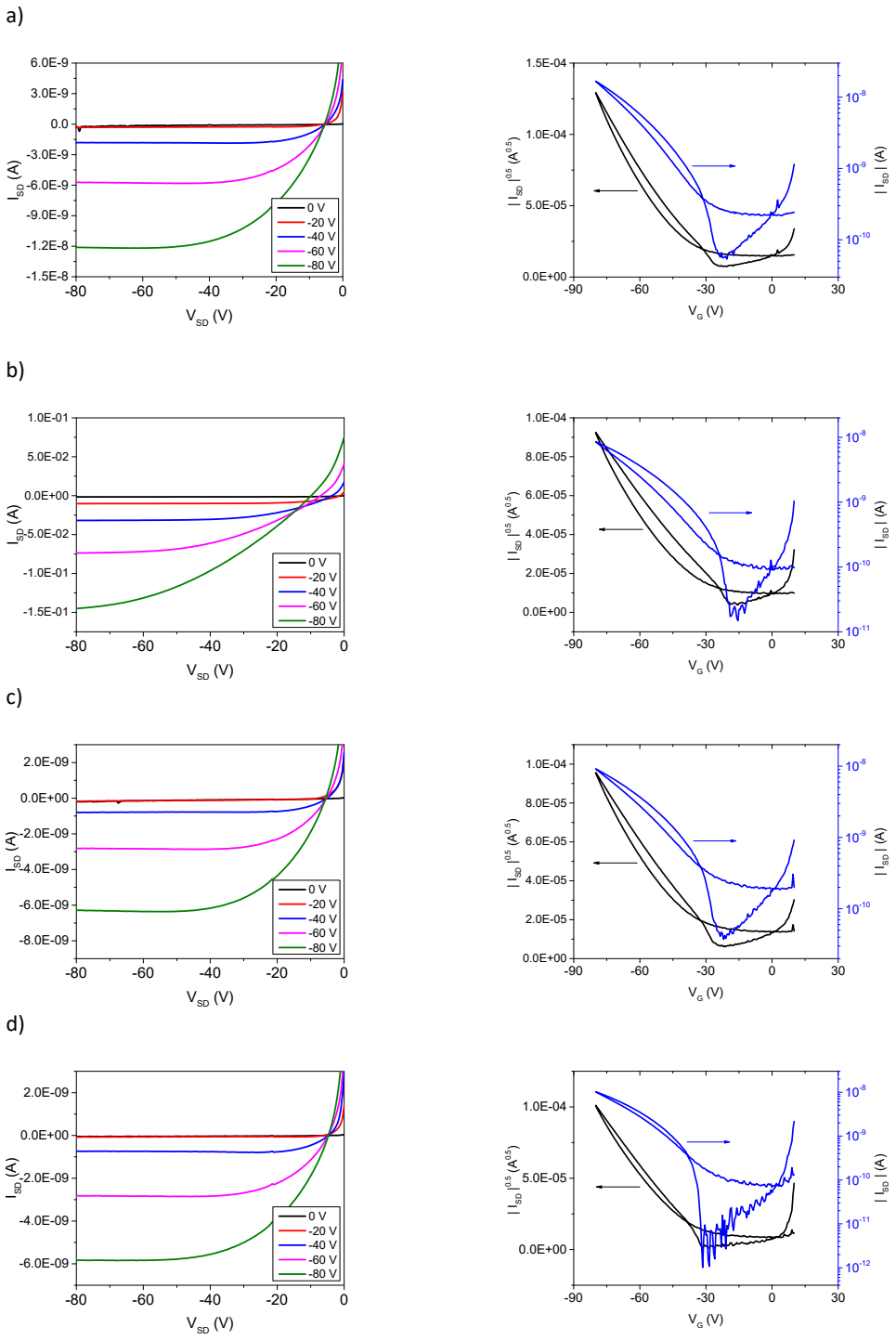

Figure S13: Representative OFET characteristics devices prepared from P3 on SiO_2. a) output (left) and transfer (right) curves for devices at a) 0%, b) 10%, c) 20% and d) 30% strain for charge transport oriented perpendicular to strain direction.

<u>Strain for charge transport oriented parallel to strain direction - **P3**</u>

a)

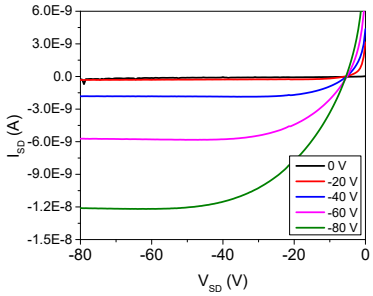

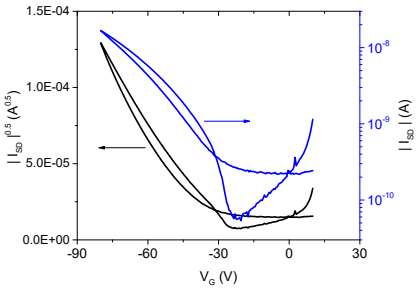

b)

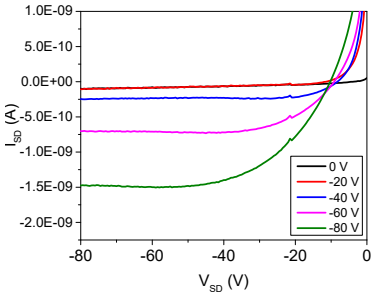

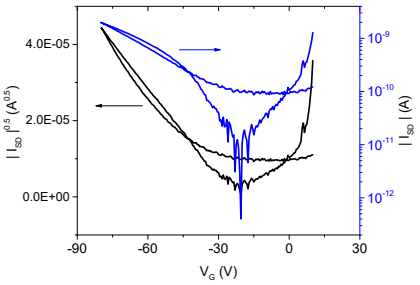

c)

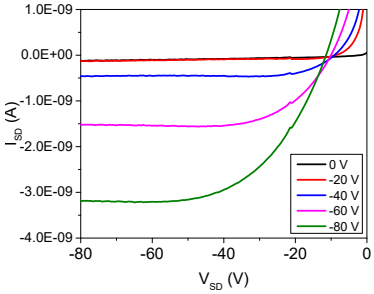

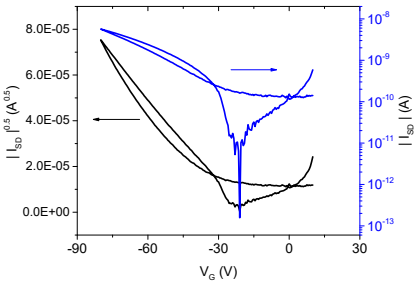

d)

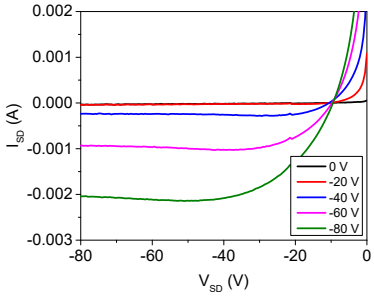

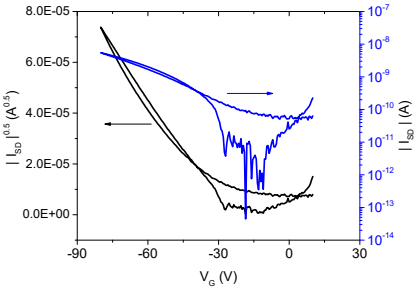

Figure S14: Representative OFET characteristics devices prepared from P3 on SiO_2. a) output (left) and transfer (right) curves for devices at a) 0%, b) 10%, c) 20% and d) 30% strain for charge transport oriented parallel to strain direction.

<u>Strain for charge transport oriented perpendicular to strain direction - **P4**</u>

a)

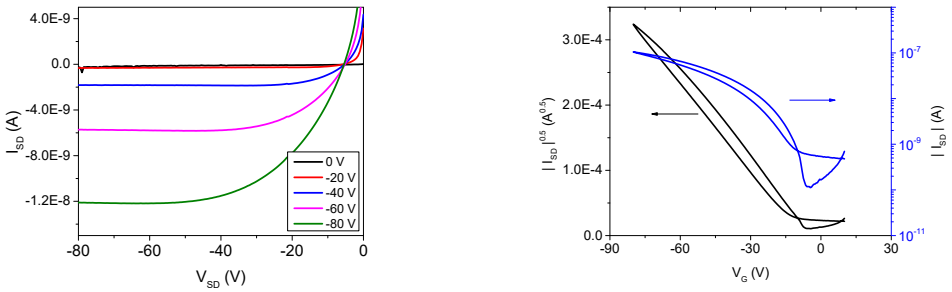

b)

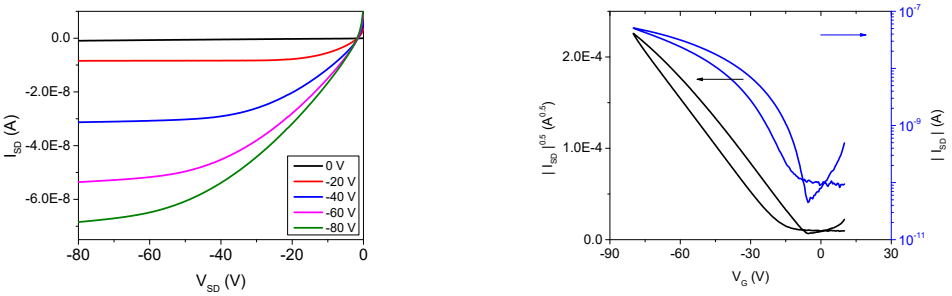

c)

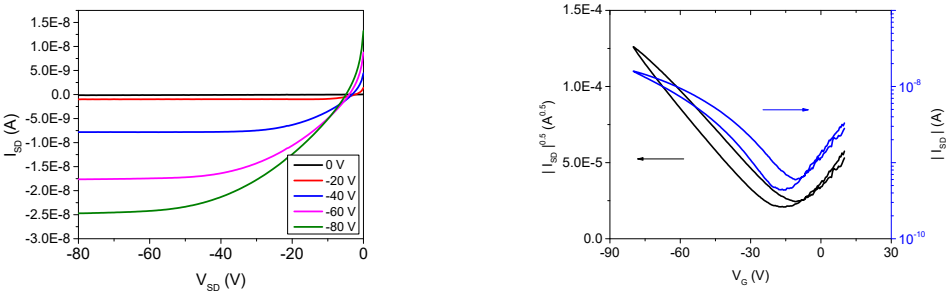

d)

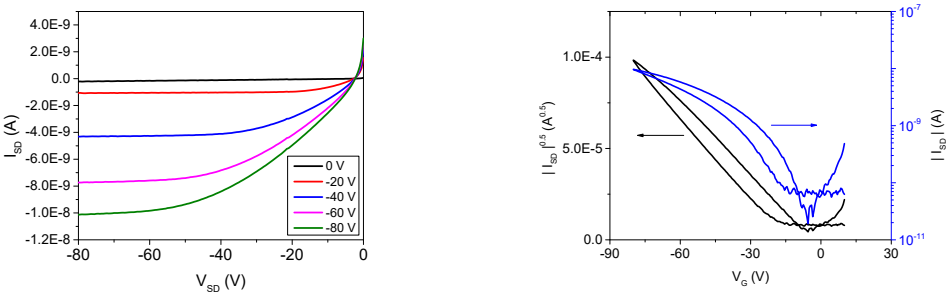

Figure S15: Representative OFET characteristics devices prepared from P4 on SiO_2. a) output (left) and transfer (right) curves for devices at a) 0%, b) 10%, c) 20% and d) 30% strain for charge transport oriented perpendicular to strain direction.

Strain for charge transport oriented parallel to strain direction - **P4**

a)

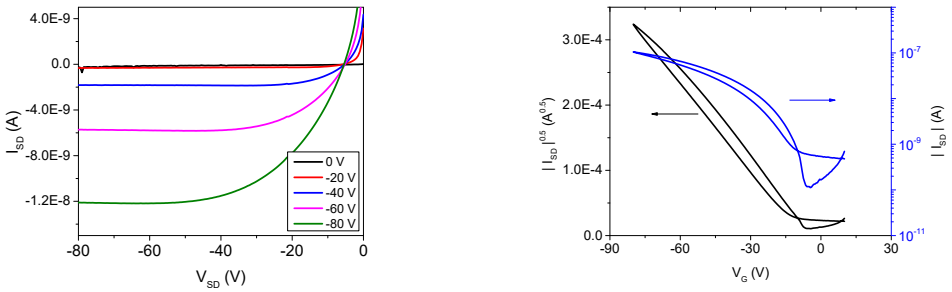

b)

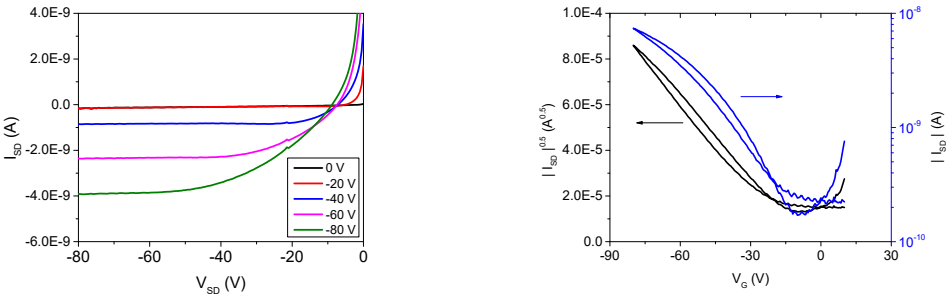

c)

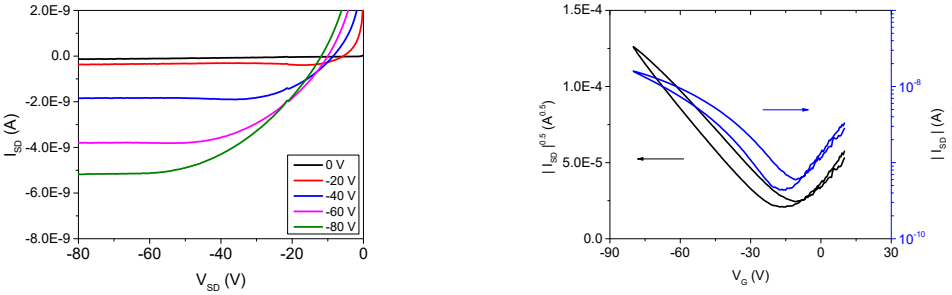

d)

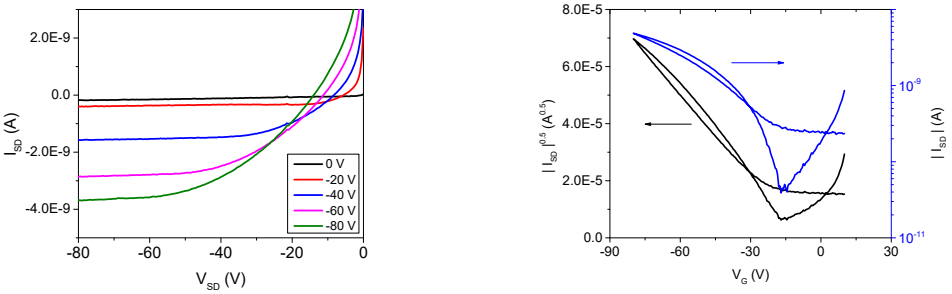

Figure S16: Representative OFET characteristics devices prepared from P4 on SiO_2. a) output (left) and transfer (right) curves for devices at a) 0%, b) 10%, c) 20% and d) 30% strain for charge transport oriented parallel to strain direction.

Polymers Thickness Measurements with Atomic Force Microscopy (AFM)

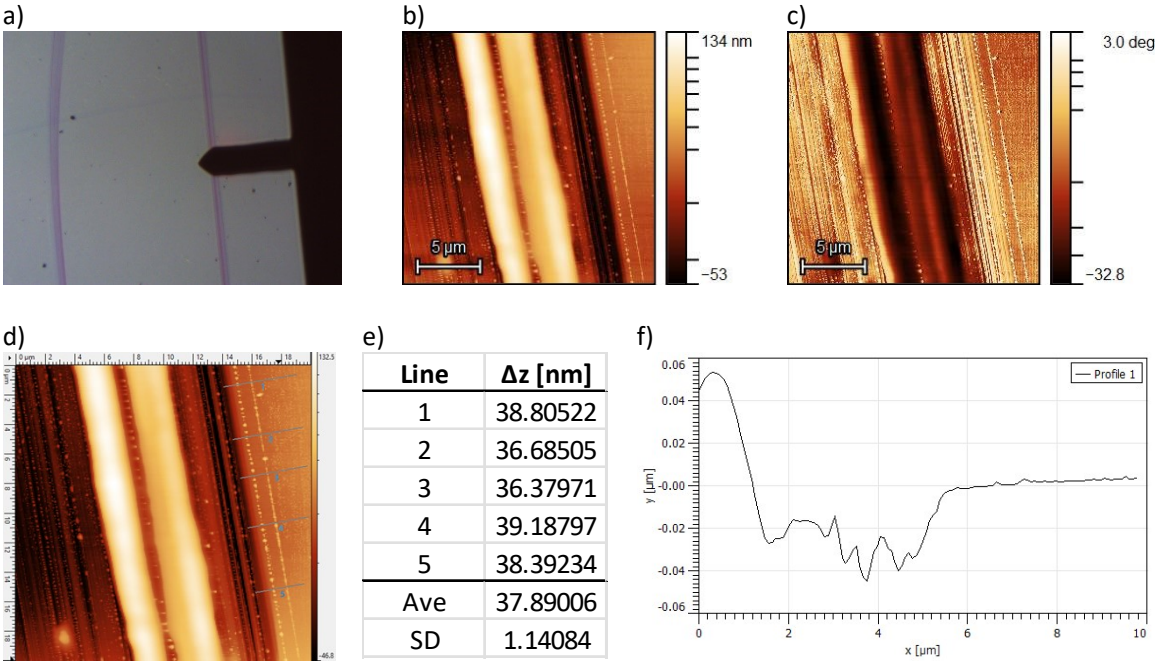

Line	Δz [nm]
1	38.80522
2	36.68505
3	36.37971
4	39.18797
5	38.39234
Ave	37.89006
SD	1.14084

Figure S17: AFM thickness measurements for thin films of **P1.** a) Optical image (10x) from the AFM camera showing the scratch where thickness is being evaluated. The purple line represents the SiO_2 wafer substrate, b) Height image, c) Phase image, d) Height image with five lines across the section to determine thickness, e) Thickness measurements, resulting in an average thickness of 37.89 ± 1.14 nm, f) Height profile image of the scratched area on the thin film.

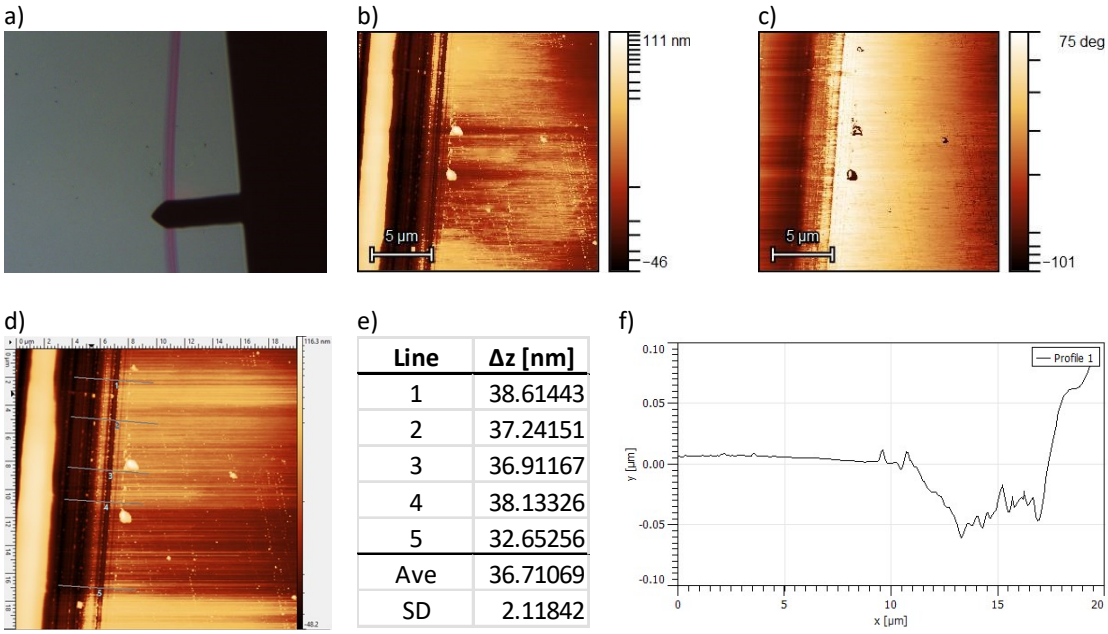

Line	Δz [nm]
1	38.61443
2	37.24151
3	36.91167
4	38.13326
5	32.65256
Ave	36.71069
SD	2.11842

Figure S18: AFM thickness measurements for thin films of **P2.** a) Optical image (10x) from the AFM camera showing the scratch where thickness is being evaluated. The purple line represents the SiO_2 wafer substrate, b) Height image, c) Phase image, d) Height image with five lines across the section to determine thickness, e) Thickness measurements, resulting in an average thickness of 36.71 ± 2.11, f) Height profile image of the scratched area on the thin film.

a)

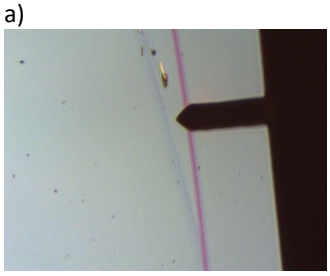

b)

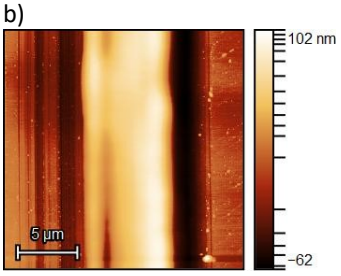

c)

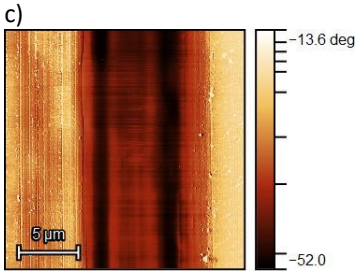

d)

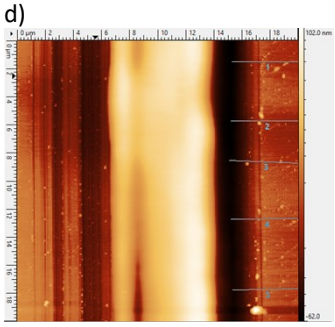

e)

Line	Δz [nm]
1	44.52394
2	44.73948
3	43.17221
4	55.65537
5	40.63404
Ave	45.74501
SD	5.166405

f)

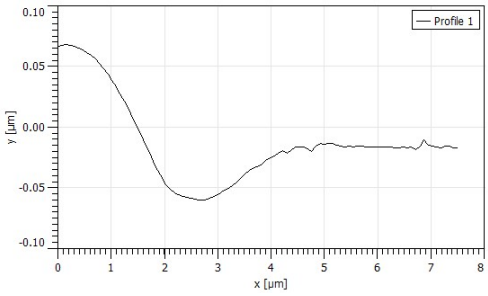

Figure S19. AFM thickness measurements for thin films of **P3.** a) Optical image (10x) from the AFM camera showing the scratch where thickness is being evaluated. The purple line represents the SiO_2 wafer substrate, b) Height image, c) Phase image, d) Height image with five lines across the section to determine thickness, e) Thickness measurements, resulting in an average thickness of 45.74 ± 5.16 nm, f) Height profile image of the scratched area on the thin film.

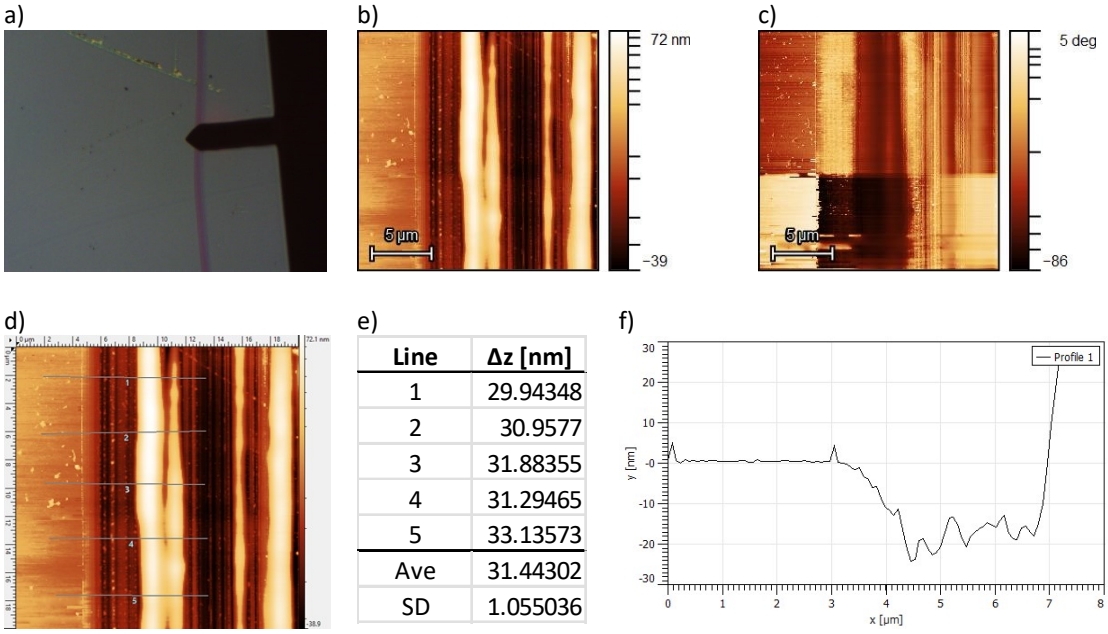

Line	Δz [nm]
1	29.94348
2	30.9577
3	31.88355
4	31.29465
5	33.13573
Ave	31.44302
SD	1.055036

Figure S20. AFM thickness measurements for thin films of **P4.** a) Optical image (10x) from the AFM camera showing the scratch where thickness is being evaluated. The purple line represents the SiO_2 wafer substrate, b) Height image, c) Phase image, d) Height image with five lines across the section to determine thickness, e) Thickness measurements, resulting in an average thickness of 31.44 ± 1.05 nm, f) Height profile image of the scratched area on the thin film.

References

1 M. Comí; D. Patra; R. Yang; Z. Chen; A. Harbuzaru; Y. Wubulikasimu; S. Banerjee; R. Ponce Ortiz; Y. Liu; M. Al-Hashimi. Alkoxy Functionalized Benzothiadiazole Based Donor-Acceptor Conjugated Copolymers for Organic Field-Effect Transistors. *J. Mater. Chem. C* 2021, **9**, 5113–5123.